INFLUENCE OF DIFFERENT RADIOMETRIC CORRECTIONS APPLIED IN OLI LANDSAT-8 IMAGES OVER BURNED AREA DETECTION IN PANTANAL BIOME

Letícia Ferrari Castanheiro[1], Vinicius Silva Werneck Orlando[1], Letícia Rosim Porto[1], Fernanda Sayuri Yoshino Watanabe[1], Maria de Lourdes Bueno Trindade Galo[1]

[1] São Paulo State University (Unesp), School of Technology and Sciences, Presidente Prudente, São Paulo, Brazil – (leticia.ferrari, vinicius.werneck, leticia.porto, fernanda.watanabe, trindade.galo)@unesp.br

ABSTRACT

Remote sensing has been shown an important technique in the identification of burned areas. However, satellite images are strongly influenced by atmosphere components and variations of illumination, which must be corrected in some applications. In this paper, we assessed the influence of image radiometric corrections in burned area detection. We downloaded Level-1 and Level-2 products from Operational Land Imager (OLI), onboard Landsat 8 satellite, taken before and after fire events occurred in Pantanal (Brazil). Three methods of radiometric correction were applied: radiometric calibration, atmospheric correction by using ACOLITE, and radiometric normalization. The Normalized Burn Ratio (NBR) spectral index was applied in images derived after each correction and Level-2 product to detect burned areas. The results were compared with fire data from the National Institute for Space Research (INPE). Level-2 images presented better-burned area detection than those derived from other methods of radiometric correction.

Key words — forest fire, change detection, radiometric calibration, atmospheric correction, Normalized Burn Ratio.

1. INTRODUCTION

Pantanal biome is the largest continuous wetlands on the planet. The clime is predominantly tropical with hot and rainy summer, and cold and dry winter. The biome is extremely rich due to the environmental conditions that benefit the presence of wildlife and biodiversity [1]. As fauna and flora are admirable, a rich culture can also be found in Pantanal, where traditional communities live, such as indigenous and quilombos.

Despite its natural beauty, the Pantanal biome has been highly affected by human activities, such as agriculture that use fire for land management. In the dry season, fires can spread without control, impacting vast areas [2]. Recently, wildfires have increased in Pantanal. Large areas of forests and the population that lives there have been affected. Furthermore, the ecosystem has been severely impacted by the loss of biodiversity and changes in biogeochemical cycles and the atmosphere [3]. Thus, burned area detection is important for fire management and understanding the effects on the ecosystem.

Remote sensing has become an important tool for fire monitoring since the variability of the spectral response of the burned surface occurs [4]. Therefore, mapping fire events have been widely studied [2] [5] [6]. Spectral indexes have been widely used to identify the interested phenomenon using images acquired in different periods. Normalized burn ratio (NBR), proposed by [7], was developed specifically to map burned areas and has presented satisfactory results [4] [5].

For reliable results, multispectral images must be radiometrically corrected, mainly for a temporal analysis that uses images from different dates. Radiometric calibration reduces the instrument effects, converting a digital number (DN) to top-of-atmosphere (TOA) radiance or reflectance. The application of atmospheric correction in satellite images is important due to the high influence of atmospheric components in the radiance registered by the sensor. Another method that allows radiometrically matching images taken at different times is radiometric normalization, which reduces the intensity variations of solar illumination.

In this work, the influence of different radiometric corrections in multispectral images on the detection of burned areas was analysed. Landsat 8/OLI images (Level-1 and Level-2 products) of a region of Pantanal biome acquired before and after the fire were used. The radiometric calibration and atmospheric correction were performed in the Level-1 product, and radiometric normalization was done in the Level-2 product. After each correction, burned areas were mapped using NBR. The results were compared to each other and with fire data from Pantanal in September/2020, provided by the National Institute for Space Research (INPE) [8].

2. DATASETS AND EXPERIMENTS

2.1. Study area and data

The study area is part of the Brazilian Pantanal biome located in Mato Grosso and Mato Grosso do Sul States (Figure 1). The region includes the National Park of Pantanal Matogrossense, which is managed by the Chico Mendes Institute for Biodiversity Conservation (ICMBio).

The experiments were performed using Level-1 and Level-2 products from Landsat 8/OLI sensor. Level-1 product is geometrically corrected, and Level-2 products are corrected of atmospheric conditions by Landsat Surface Reflectance Code (LaSRC – [9]). Considering the weather variability over a year in Pantanal, the images before (pre-fire) and after (post-fire) the fire were chosen with 1 year of difference (pre-fire: 10/09/2019; post-fire: 12/09/2020).
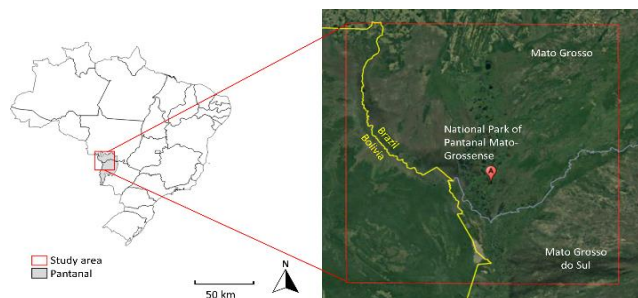
Figure 1. Study area: Pantanal Matogrossense.

2.2. Corrections of multispectral image

The radiometric calibration was applied in pre- and post-fire Level-1 images in the QGIS software. The conversion of digital number (DN) to TOA reflectance was performed with a linear model, whose parameters are provided in the image metadata. The atmospheric correction of Level-1 products was performed using atmospheric correction for OLI 'lite' (ACOLITE – [10]). ACOLITE is a scene-based method, while LaSRC (Land Surface Reflectance Code) is based on the radiative transfer model, which generates surface reflectance (Level-2 products). The radiometric normalization was performed using Level-2 images, in which the pre-fire image was considered as reference data. The reflectance values of the five darkest pixels and five brightest pixels were used to estimate the coefficients of a linear transformation [11]. The radiometric normalization was conducted only for near-infrared (NIR) and shortwave infrared 2 (SWIR$_2$) bands, used in NBR. Therefore, four types of images were used in the next step: (1) radiometrically calibrated images (images$_{RC}$); (2) atmospherically corrected images with ACOLITE (images$_{ACOLITE}$); (3) Level-2 images (images$_{Level2}$); and (4) radiometrically normalized Level-2 images (images$_{RN}$).

The resultant images of each method were compared to each other considering the reflectance spectra of vegetation and water for the spectral bands: blue, green, red, NIR, shortwave infrared 1 (SWIR$_1$), and SWIR$_2$. Since, radiometric normalization was performed only for NIR and SWIR$_2$, a further comparison was done between ACOLITE and LaSRC atmospheric correction.

2.3. Burned area detection

NBR is used to highlight the burned areas, while dNBR is applied to classify the severity of the fire. NBR uses images from NIR and SWIR$_2$ channels (Equation 1), which have less influence on smoke from burning. In addition, the gradient between the NIR and SWIR varies with the loss of vegetation and moisture. NBR was applied in the pre- and post-fire images of each product mentioned in Section 2.2. Then, the burned areas were detected by calculating the difference NBR (dNBR) (Equation 2).

After that, dNBR images were classified to analyse the fire severity in the study area. The classification of severity was performed following the criteria in Table 1 [7]. This procedure was performed for images$_{RC}$, images$_{ACOLITE}$, images$_{level2}$, and images$_{RN}$. The classified images were compared with the burning data of Pantanal provided by INPE.

$$NBR = \frac{NIR - SWIR_2}{NIR + SWIR_2} \qquad (1)$$

$$dNBR = NBR_{pre} - NBR_{post} \qquad (2)$$

Severity level	dNBR
High regeneration	-500 to -250
Low regeneration	-251 to -100
No burned	-101 to 99
Low severity	100 to 269
Low moderate severity	270 to 439
High moderate severity	440 to 659
High severity	660 to 1350
Anomaly	> 1350

Table 2. Fire severity classification based on Key and Benson (1999). dNBR values were multiplied for 10^3.

3. RESULTS AND DISCUSSIONS

The reflectance spectra were not compared for the radiometrically normalized images, because this procedure was performed only for NIR and SWIR$_2$ bands. Figure 2 shows the linear regression obtained for NIR (B5) and SWIR$_2$ (B7).
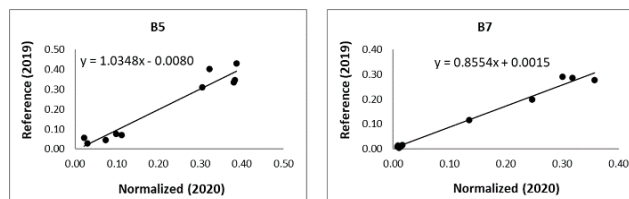

Figure 2. Linear regression for radiometric normalization of NIR (B5) and SWIR$_2$ (B7) bands.

Reflectance spectra were generated to compare images treated with radiometric calibration (ρ sensor TOA), atmospheric calibration with ACOLITE (ρ surface ACOLITE) and Level-2 products (ρ sup. Level 2). The comparison was done for water and vegetation targets considering pre- and post-fire images (2019 and 2020, respectively). Figure 3 shows the reflectance spectra for (a) vegetation and (b) water targets, considering the spectral bands: blue (B2), green (B3), red (B4), NIR (B5), SWIR$_1$ (B6), and SWIR$_2$ (B7).

In Figure 3a, the reflectance values obtained from images (2019 and 2020) with only radiometric correction did not represent the standard spectral curve for both vegetation and water, mainly in the visible bands (2, 3 and 4). The atmosphere components cause more scattering at short wavelengths, increasing the reflectance values.

Improvements can be seen when performing the

atmospheric correction with ACOLITE. However, the reflectance values of vegetation and water in the visible bands of the post-fire image (2020) presented different behaviour compared with the pre-fire image (2019). This occurs likely due to the presence of smoke from burning in the scene, in which short wavelengths are more affected. The Level-2 images presented more consistent reflectance spectra for both targets. Furthermore, the atmospheric correction technique used to generate the Level-2 images (LaSRC) is more robust than ACOLITE. The difference can be seen in Figure 4, which shows images of the red band with (a) ACOLITE and (b) LaSRC atmospheric corrections. In Figure 4a, there is smoke in the scene, while there is not in Figure 4b.
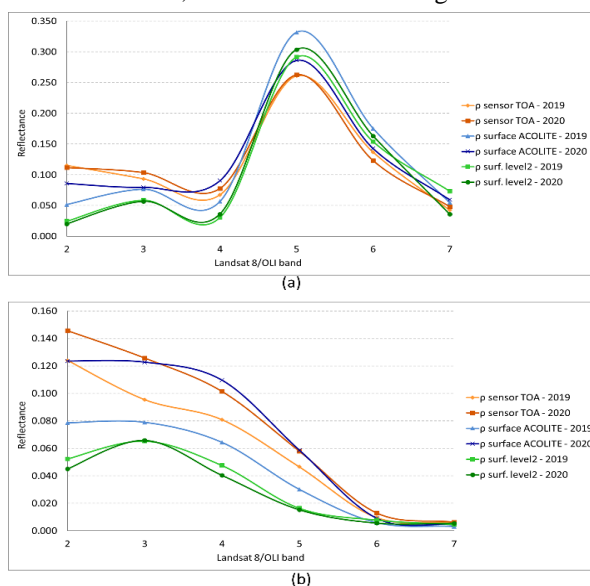

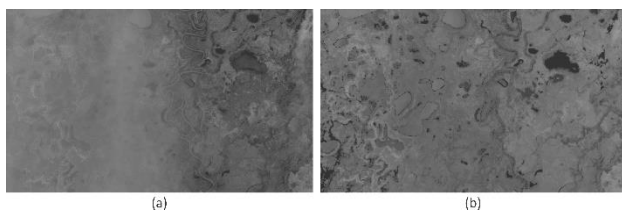**Figure 3. Spectral curves for (a) vegetation and (b) water.**

Figure 4. Comparison of atmospheric corrections: (a) ACOLITE and (b) LaSRC.

Despite the smoke from burning presented in the scene, the infrared bands (NIR and SWIR) are not influenced by this smoke, which are the bands used in the NBR index. Therefore, the NBR spectral index was applied to the pre- and post-fire images after each correction.

Figure 5 presents the fire severity classification in the dNBR images obtained from (a) images$_{RC}$ (b) images$_{ACOLITE}$ (c) images$_{level-2}$, (d) images$_{RN}$. Comparing the classifications presented in Figure 5, more regenerated and no-burned areas are presented in Figure 5a than Figure 5b. The atmospheric correction minimizes the scattering caused by atmosphere components, which can influence the performance of the classification. The classification with images$_{ACOLITE}$ (Figure

5b) and images$_{level\ 2}$ (Figure 5c) presented similar results. Some differences were noticed in the classification of water bodies. In Figure 5b, some of them were classified as regeneration, while as no burned area in Figure 5c. Considering that the images before and after the fire were chosen with a year of difference, the illumination of both scenes has a slight variation. Therefore, Figure 5c and Figure 5d presented similar results, with small differences in the severity levels.
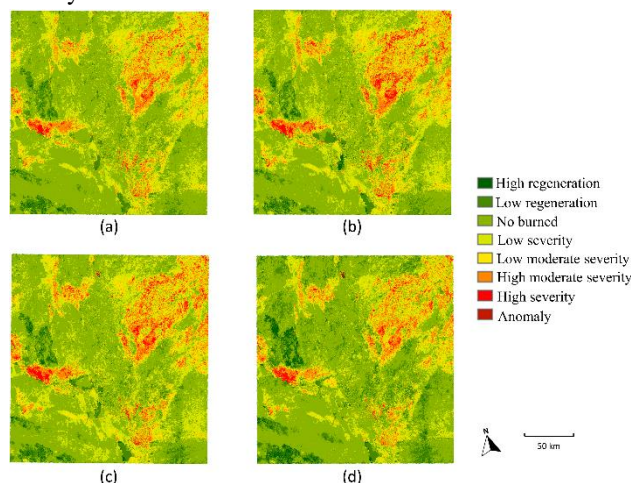

Figure 5. Classification of burned areas on (a) images$_{RC}$, (b) images$_{ACOLITE}$, (c) images$_{level\ 2}$, (d) images$_{RN}$.

The areas with low severity can be bare soil due to deforestation or burned areas from a time ago. In Figure 5, the burned areas were represented by red tones. The dark red indicates an anomaly, which can be caused by atmospheric effects or unreal changes in land cover [12]. In this work, anomalies were identified as fire in the instant the image was taken, which is illustrated in Figure 6. Figure 6a shows the anomaly (dark red) in the classification of images$_{ACOLITE}$. This anomaly also appears in another classification. In Figure 6b, the fire with smoke presented in the scene can be seen in the local and was classified as an anomaly. The image presented in Figure 6b is a composition of red, NIR and SWIR$_2$ (RGB-457).
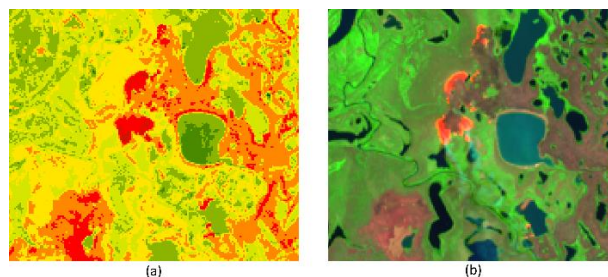

Figure 6. Anomaly classification of fires presented in the scene.

Misclassification can be observed for water bodies, which were classified as burned or regeneration areas while should be no burned area. Figure 7 presents water bodies in the classified images obtained from (a) images$_{RC}$ (b) images$_{ACOLITE}$ (c) images$_{level\ 2}$ and (d) images$_{RN}$. In Figure 7a

and Figure 7b, the lake was classified as low regeneration. In Figure 7c and Figure 7d, some parts of the water were classified as burned areas. Considering that Pantanal is a wetland, the vegetation may be under the water on the date of acquisition of the post-fire image, causing confusion in the classification. [12] minimized this mistake by using another spectral index to detect water [13].
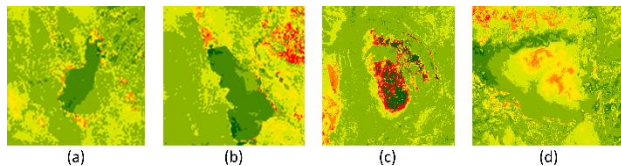

Figure 7. Classification of water bodies as regeneration and burned areas in (a) imagesRC (b) imagesACOLITE (c) imageslevel 2 and (d) imagesRN.

These classifications were compared to fire data from INPE. Figure 8 shows in (a) the distribution of the detected fires (red points) in September/2020, available in the INPE database, superimposed on the classification result of: (b) imagesRC (c) imagesACOLITE (d) imageslevel 2, (e) imagesRN. The most burned areas were correctly classified when compared with the data from INPE (Figure 8). Some areas that were classified as burned, but did not have points of detected fire, have been probably burned before September.
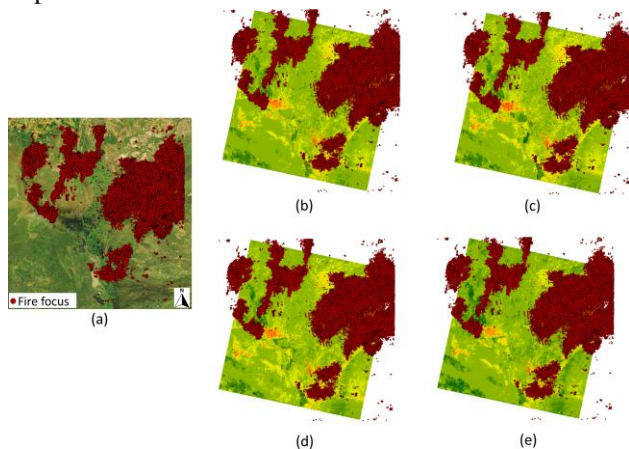

Figure 8. (a) Detected fires in September/2020 provided by INPE, on the classification of (b) imagesRC (c) imagesACOLITE (d) imageslevel 2, (e) imagesRN.

5. CONCLUSION

This paper presented a study of the influence of image corrections on burned area detection and fire severity classification. The corrections were: the radiometric calibration, atmospheric correction (ACOLITE and Level-2 image) and radiometric normalization. The results showed the importance of a suitable correction in the images, mainly the atmospheric correction. The Level-2 image presented a better correction of atmospheric components, which uses the LaSRC.

The classifications presented match compared to the fire data of Pantanal provided by INPE. Some misclassifications were identified, such as water bodies classified as burned areas. This problem can be minimized using the spectral index as Normalized Difference Water Index (NDWI) [13], which detects the water bodies. Another spectral index to identify burned areas, such as CBI (composite burn index), can be tested and compared to NBR. The radiometric normalization with linear regression did not present significant improvements, therefore, other radiometric normalization methods are recommended to be tested.

7. REFERENCES

[1] M. B. Harris, W. Tomas, G. Mourão, C. J. Da Silva, E. Guimaraes, F. Sonoda, and E. Fachim. Safeguarding the Pantanal wetlands: threats and conservation initiatives. *Conservation Biology*, 19(3), 714-720. 2005.

[2] R. Libonati, C. C. Da Camara, A. W. Setzer, F. Morelli, and A. E. Melchiori. An algorithm for burned area detection in the Brazilian Cerrado using 4 µm MODIS imagery. *Remote Sensing*, 7(11), 15782-15803. 2015.

[3] J. F. Marques, M. B. Alves, C. F. Silveira, A. A. e Silva, T. A. Silva, V. J. Dos Santos, and M. L. Calijuri. Fires dynamics in the Pantanal: Impacts of anthropogenic activities and climate change. *Journal of Environmental Management*, *299*, 113586. 2021.

[4] T. Loboda, K. J. O'neal, and I. Csiszar, Regionally adaptable dNBR-based algorithm for burned area mapping from MODIS data, *Remote Sensing of environment*, v. 109, n. 4, p. 429-442. 2007.

[5] M. G. Franco, I. A. Mundo, and T. T. Veblen. Field-validated burn-severity mapping in north Patagonian forests, *Remote Sensing*, v. 12, n. 2, p. 214. 2020.

[6] M. M. Pinto, R. Libonati, R. M. Trigo, I. F. Trigo, and C. C. DaCamara. A deep learning approach for mapping and dating burned areas using temporal sequences of satellite images. ISPRS Journal of Photogrammetry and Remote Sensing, 160, 260-274. 2020.

[7] C. H. Key, and N. C. Benson. Measuring and remote sensing of burn severity, *Proceedings joint fire science conference and workshop*, 2: 284. 1999.

[8] Instituto Nacional de Pesquisas Espaciais (INPE). *Banco de Dados Queimadas*. Disponível em: < https://queimadas.dgi.inpe.br/queimadas/bdqueimadas>. Acesso em: 05 set. 2022.

[9] E. Vermote, C. Justice, M. Claverie, and B. Franch. Preliminary analysis of the performance of the Landsat 8/OLI land surface reflectance product. *Remote Sensing of Environment*, 185, 46-56. 2016.

[10] Q. Vanhellemont, and K. Ruddick. Turbid Wakes Associated with Offshore Wind Turbines Observed with Landsat 8. *Remote Sensing of Environment*, 145, 105–115. 2014.

[11] F. G. Hall, D. E. Strebel, J. E. Nickeson, and S. J. Goetz. Radiometric rectification: toward a common radiometric response among multidate, multisensor images, *Remote Sensing of Environment*, 35(1): 11-27. 1991.

[12] T. M. Rosan, and E. Alcântara. Detecção de áreas queimadas e severidade a partir do índice espectral ΔNBR. In: In: Simpósio Brasileiro de Sensoriamento Remoto, 17. Anais... João Pessoa, 2015. p. 526-533.

[13] S. K. McFeeters. The use of the Normalized Difference Water Index (NDWI) in the delineation of open water features. International Journal of *Remote Sensing*, v.17, n.7, p.1425-1432, 1996.